Electronic Supplementary Material (ESI) for Journal of Materials Chemistry A.

Supplementary Information

Hydrazide and amidoxime dual functional membranes for uranium extraction from seawater

Yunyou Yao[a], Jian Liao[b], Xiao Xu[a], Chen Huang[a], Mengtao Fu[a], Kang Chen[a], Lin Ma[c], Jiaguang Han[b], Lu Xu[c*], Hongjuan Ma[a*]

a Shanghai Applied Radiation Institute, Shanghai University, Shanghai, 200444, China.

b College of Ocean Engineering and Guangxi Key Laboratory of Optoelectronic Information Processing, Guilin University of Electronic Technology, Beihai 536000, China

c Shanghai Institute of Applied Physics, Chinese Academy of Sciences, Shanghai 201800, China.

* Corresponding author:

Lu Xu: xulu@sinap.ac.cn;

Hongjuan Ma: hongjuanma@shu.edu.cn

1. Experimental section

1.1 Characterization methods

Fourier-transform infrared (FT-IR) spectra were collected on a Nicolet Avatar 370 FTIR spectrometer (Thermo Nicolet Company, USA) in attenuated total reflectance mode with a resolution of 4 cm^{-1} and 16 scans. The elemental composition and chemical states of the membranes were analyzed by X-ray photoelectron spectroscopy (XPS) using a Thermo SCIENTIFIC ESCALAB 250Xi instrument. The XPS data were acquired through wide scans ranging from 0 to 1300 eV. In order to analysis of the hydrazide density of PE-PAO@ADH membrane. The absorbance of each mixed ADH and BCA solution were collected on an Ultraviolet visible light photometer (PerkinElmer, Lambda 265).

TGA was performed (NETZSCH, TG209, F3) in the temperature range from 25 to 800°C with a heating rate of 10 °C per minute under a nitrogen flow. Mechanical tests were conducted on a universal material testing machine (TIDJ-1000, Suzhou Zhuo Xu Precision Industry Co. Ltd., China). Nitrogen adsorption–desorption isotherms were measured by a surface aperture adsorption instrument (ASAP2010C, Micromeritics). The specific surface areas of the samples were calculated using Brunauer–Emmett–Teller (BET) method within a relative pressure (P/P0) range of 0.0–1.0, and the pore size distribution were calculated by the Barret–Joyner–Halenda (BJH) algorithm.

The surface and cross-sectional morphologies of the membrane samples and the energy dispersive spectroscopy (EDS) analysis was performed using field-emission scanning electron

microscopy (SEM) (JSM-6700F, JEOL, Japan). All the membranes were frozen and cracked in liquid nitrogen to investigate the original cross-section morphologies. All the membrane samples were sputtered with gold to enhance the electron conductivity before observation by SEM.

Contact angle experiment was used to analyze the hydrophilic and hydrophobic properties of materials by a KSV Instrument. The samples were fixed upon the specimen stage. A drop of 5 μL distilled water was dropped onto the surface of the sample. Photographs were recorded with a NAVITAR camera to analyze the contact angle. The angle of the contact point between water droplets and the sample surface was regarded as the contact angle of the sample. Each sample was measured five times at different locations of the surface. The concentrations of U and other metals were analyzed by Inductively Coupled Plasma Mass spectrometry (ICP-MS, NexION 300D) and an Atomic Emission Spectrometer (ICP-AES, Optima 8000).

1.2 Synthesis of PE-PAO@ADH membranes and calculation

PE membranes were used as the trunk material for preparing the PE@ADH, PE-PAO and PE-PAO@ADH membranes. Before irradiation, the PE membrane was placed in a flask containing a monomer solution of AA/AN/DMF (8 vol%/32 vol%/60 vol%) and then purged with nitrogen gas for 15 min to remove the oxygen. At room temperature, the PE membrane was co-irradiated with mixed monomer solutions using electron beam (EB), the absorbed dose range of 40 to 200 kGy. Finally, the polyacrylonitrile and polyacrylic acid co-grafted PE-*g*-(PAN-*co*-PAA) membrane was extracted with DMF, washed with H_2O and ethanol to remove

homopolymers and residual monomers and dried in an oven at 60 °C. The degree of grafting (DG) of the PE-*g*-(PAN-*co*-PAA) membrane was calculated as follows:

$$DG(\%) = \frac{M_1 - M_0}{M_0} \times 100\% \qquad (S1)$$

where M_0 is the weight of the original PE membrane, and M_1 is the weight after grafting.

Subsequently, a solution containing $NH_2OH{\cdot}HCl$ at a concentration of 10 wt% was prepared by employing a bicomponent solvent comprising H_2O (50 vol%) and methanol (50 vol%). The NaOH solution was used to adjust the pH of the solution to a neutral state. The PE-*g*-(PAN-*co*-PAA) membranes were placed in $NH_2OH{\cdot}HCl$ at 70 °C for 24 hours to convert the nitrile groups into the AO groups. After obtaining the PE-PAO membrane, it was washed with deionized water to remove NH_2OH that had not been reacted, and then dried in a vacuum oven at 60 °C. The density of the AO group in the PE-PAO membrane was ascertained through the utilization of the subsequent equation:

$$AO\ Density\left(\frac{mmol}{g}\right) = \frac{(M_3 - M_2) \times 1000}{33 \times M_3} \qquad (S2)$$

where M_2 and M_3 represent the weights of PE-*g*-(PAN-*co*-PAA) and PE-PAO membrane, correspondingly, while 33 is the the molecular weight of the AO group subtracted by the molecular weight of the nitrile group.

The hydrazide-functionalized PE-PAO@ADH membranes were synthesized with the formation of amide bonds between the carboxyl groups of PE-PAO and the hydrazide groups of ADH via the amide condensation reaction. Typically, PE-PAO and HATU were immersed in DMF at room temperature. Following 10 minutes of stirring, ADH and DIPEA were added

to the above DMF solution. The reaction solution was continuously vortexed for another two days at room temperature. The resulting PE-PAO@ADH membrane was washed with DMF and ethanol, followed by drying in a vacuum oven at 60 °C. Unlike the PE-PAO@ADH preparation process, PE-*g*-(PAN-*co*-PAA) membrane was directly subjected to the amide condensation reaction to obtain PE@ADH membrane.

The density of hydrazide groups on PE-PAO@ADH was quantified by UV spectrometer. A standard BCA reagent was obtained by mixing liquid A and liquid B in a ratio of 50:1 (v/v) according to instruction. In a typical procedure, ADH solutions were respectively added into BCA reagents. The solutions were afterward gently shaken at 37 °C for 30 min. Meanwhile, PE-PAO@ADH membrane respectively reacted with BCA reagent with constant shaking at 37 °C for 30 min. The absorbance of both ADH and BCA solutions was determined to be 562 nm. According to the relationship between the absorbances of these mixed ADH and BCA solutions and the amounts of hydrazide groups on ADH, a linear calibration curve was obtained. Then the absorbance of each collected supernatant was also measured at 562 nm. The concentration of hydrazide groups on the PE-PAO@ADH membrane was determined by comparing it to the calibration curve.

$$Hydrazide\ Density\left(\frac{\mu mol}{g}\right)=\frac{k\cdot A\cdot V}{118\times m} \quad (S3)$$

where k is the constants obtained from the calibration curve about concentration versus absorbance, A is the absorbance, V is the volume of solution, m is the quality of membrane, and 118 is the molecular weight of ADH.

1.3 Simulated seawater screening and reusability of PE-PAO and PE-PAO@ADH membranes

5 L of simulated seawater was configured for batch adsorption and six adsorption-desorption cycles. First, 175 g of sea salt was dissolved in 5 L deionized water. Next, some uranium and competing ion standard solutions were added to the 5 L solution. The initial concentrations of the uranium and competing metal ions VO^{3-}, Fe^{3+}, Co^{2+}, Ni^{2+}, Cu^{2+}, Zn^{2+}, and Pb^{2+} in the simulated seawater system were about 100 times higher than that in natural seawater. The pH value was adjusted to 8.0 ± 0.1 with 0.25 g of Na_2CO_3. Before adsorption, the membrane was conditioned by adding 0.02 g to a flask containing 50 mL of 2.5% KOH at 50 °C for 0.5 h and was washed with deionized water until the pH of the excess water in the membrane was neutral. Next, approximately 0.02 g of the membrane was added to 5 L of simulated seawater. The adsorption experiment was conducted on a rotary shaker at 26 °C and 120 rpm for 24 h. After the adsorption, the uranium and competing metal ions loaded onto the membrane were eluted with 0.1 M HCl solution at room temperature with a rotary shaker at 100 rpm for 30 min. The concentration of the eluted uranium was analyzed by ICP-OES with an appropriate dilution. The adsorption capacity of the PE-PAO and PE-PAO@ADH membranes for metal ions could be determined using the following equation:

$$Q = \frac{C \cdot V}{M} \quad (4)$$

where Q (mg/g) is the adsorption capacity of the metal ions from PE-PAO and PE-PAO@ADH membranes, C (mg/L) is the metal ion concentration measured by ICP-AES, V

(L) is the eluted solution volume, and M (g) is the weight of the dried PE-PAO and PE-PAO@ADH membrane that was used. After elution, the PE-PAO and PE-PAO@ADH membranes were immersed in 0.1 M NaOH solution at room temperature for 30 min for regeneration. Then they have rinsed with deionized water until the pH of the excess water in the PE-PAO and PE-PAO@ADH membranes was neutral. The adsorbent was used for the next adsorption–desorption cycle following the same procedure described above.

1.4 The calculation of adsorption model

The solid-liquid ratio for adsorption experiments was 0.01 g of adsorbent in 1 L of uranyl solution. The adsorption experiment was conducted on a rotary shaker at 26 °C and 120 rpm for 24 h. To study the mechanism of uranium adsorption, the experimental kinetic data of the PE-PAO and PE-PAO@ADH membranes for uranium adsorption were simulated using the following pseudo-first-order and pseudo-second-order models.

$$\ln\left(Q_e - Q_t\right) = lnQ_e - k_1 t \qquad (S5)$$

$$\frac{t}{Q_t} = \frac{1}{k_2 \cdot Q_e^2} + \frac{t}{Q_e} \qquad (S6)$$

where Q_t (mg/g) and Q_e (mg/g) are the uranium adsorption capacities at time t and equilibrium time, respectively; t is the contact time (h); k_1 and k_2 represent the kinetic rate constants of the pseudo-first-order (/h) and pseudo-second-order models, respectively (g/(mg.h)).

To further clarify the uranium adsorption mechanism of the PE-PAO@ADH membrane, the Langmuir and Freundlich equilibrium models were employed to fit the experimental data using eqs. (S7) and (S8), respectively:

$$\frac{C_e}{Q_e} = \frac{C_e}{Q_m} + \frac{1}{K_L Q_m} \quad (S7)$$

$$\ln Q_e = lnK_F + \frac{1}{n}\ln C_e \quad (S8)$$

where Q_e is the uranium adsorption capacity at equilibrium (mg/g), C_e is the equilibrium concentration of uranium (mg/L), Q_m is the maximum uranium-adsorption-capacity or saturation capacity at complete monolayer coverage (mg/g), K_L is the Langmuir adsorption constant, which represents the affinity between the adsorbates and adsorbents (L/mg), and K_F and n are the Freundlich constants characteristic of a particular adsorption isotherm (L/g).

1.5 Uranium adsorption in natural seawater

Natural seawater from the coastal area of Sanya, Hainan Province, China, was used for adsorption tests. 0.01 g of PE-PAO and PE-PAO@ADH membranes was added to 25 L of natural seawater, the container was shaken constantly at 120 rpm at room temperature, and samples were periodically collected using a pipette for about 30 d. ICP-MS was used for quantitative analysis. Seawater standards of CASS-6 (seawater), supplied by the National Research Council of Canada, were used for seawater quality-control experiments. High-purity nitric acid (2%) was used as the sample diluent and carrier phase. The uranium adsorption capacity of the PE-PAO and PE-PAO@ADH membranes could be determined using the following equation:

$$Q = \frac{(C_0 - C_t) \cdot V}{M} \quad (S9)$$

where Q (mg/g) is the uranium adsorption capacity of the membranes, C_0 and C_t (mg/L) are the concentration of uranium before and after adsorption, respectively, V (L) is the seawater

143 volume, and M (mg) is the weight of the dried membranes before adsorption.

144 **2. Supplementary Figures S1-S7**

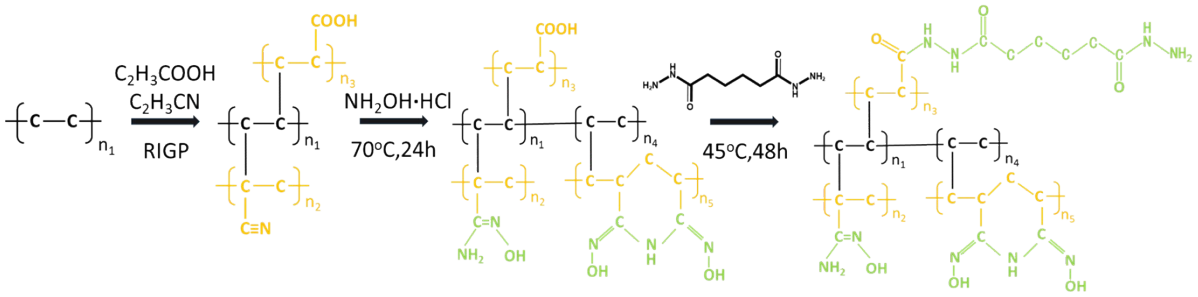

145

146 Fig. S1. Structural changes of PE, PE-*g*-(PAN-*co*-PAA), PE-PAO and PE-PAO@ADH.

147

148

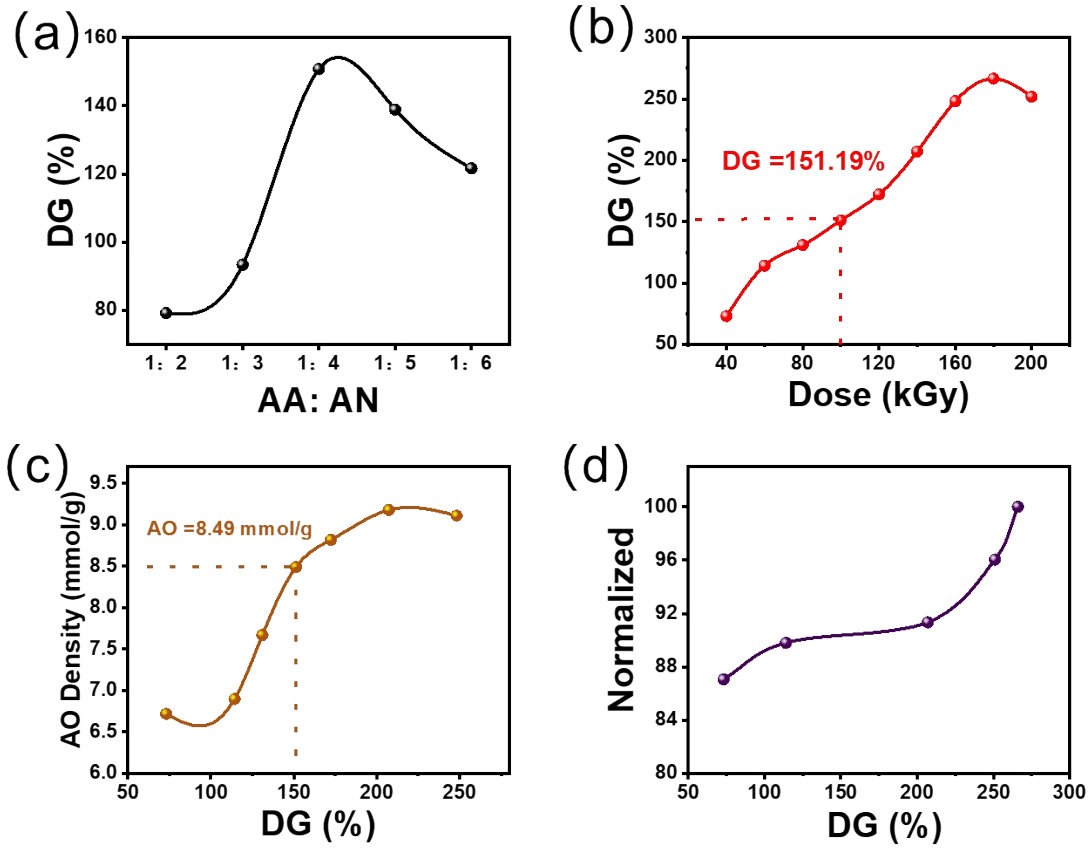

149

150 Fig. S2. DG of the PE-*g*-(PAN-*co*-PAA) membranes as a function of (a) AA: AN and (b)

151 absorbed dose. (c) AO density of the PE-PAO membranes as a function of DG. (d)

Normalized carbonyl FT-IR peaks intensity of the PE-*g*-(PAN-*co*-PAA) membranes as a function of DG.

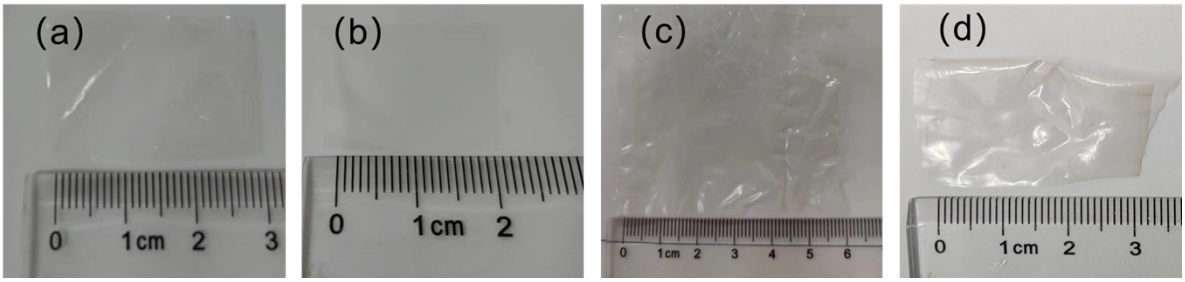

Fig. S3. Photo of (a) PE, (b) PE-*g*-(PAN-*co*-PAA)，(c) PE-PAO and (d) PE-PAO@ADH membranes.

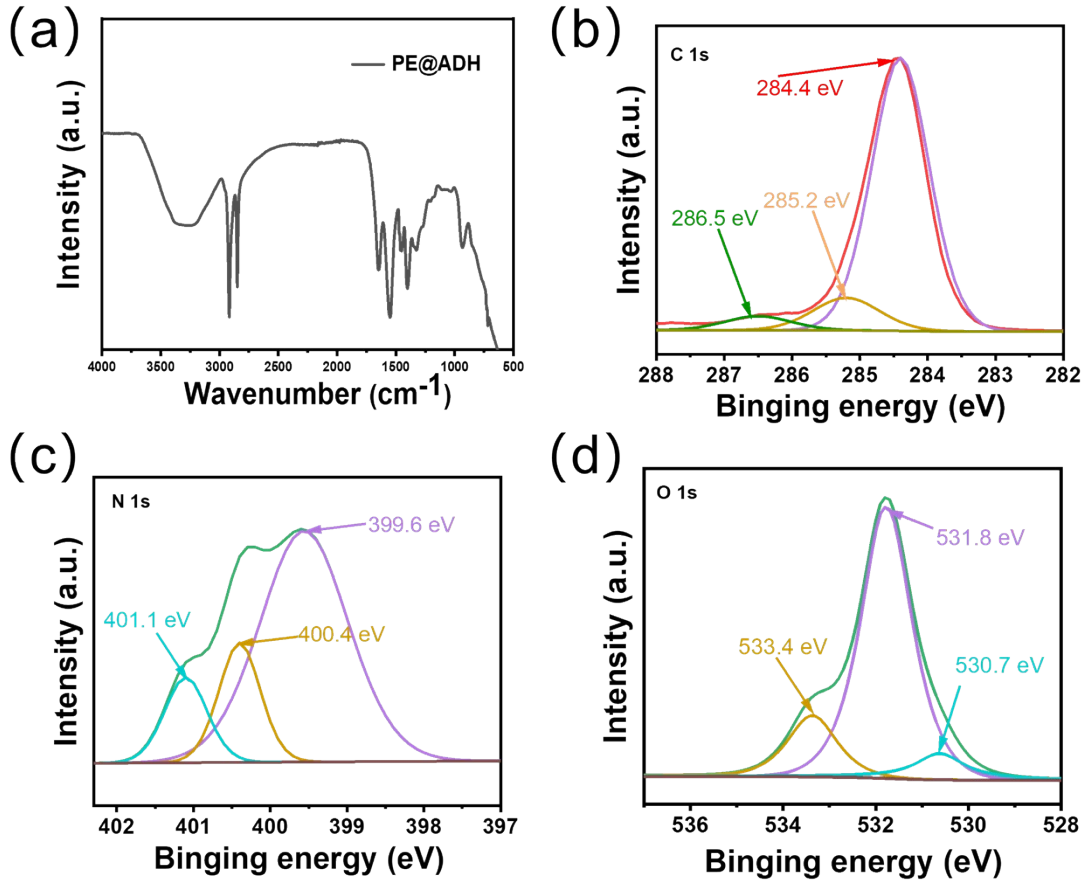

Fig. S4. Characterization of PE@ADH membranes. (a) FT-IR spectra. High-resolution XPS analysis of (b) carbon, (c) nitrogen, and (d) oxygen of PE @ADH membranes.

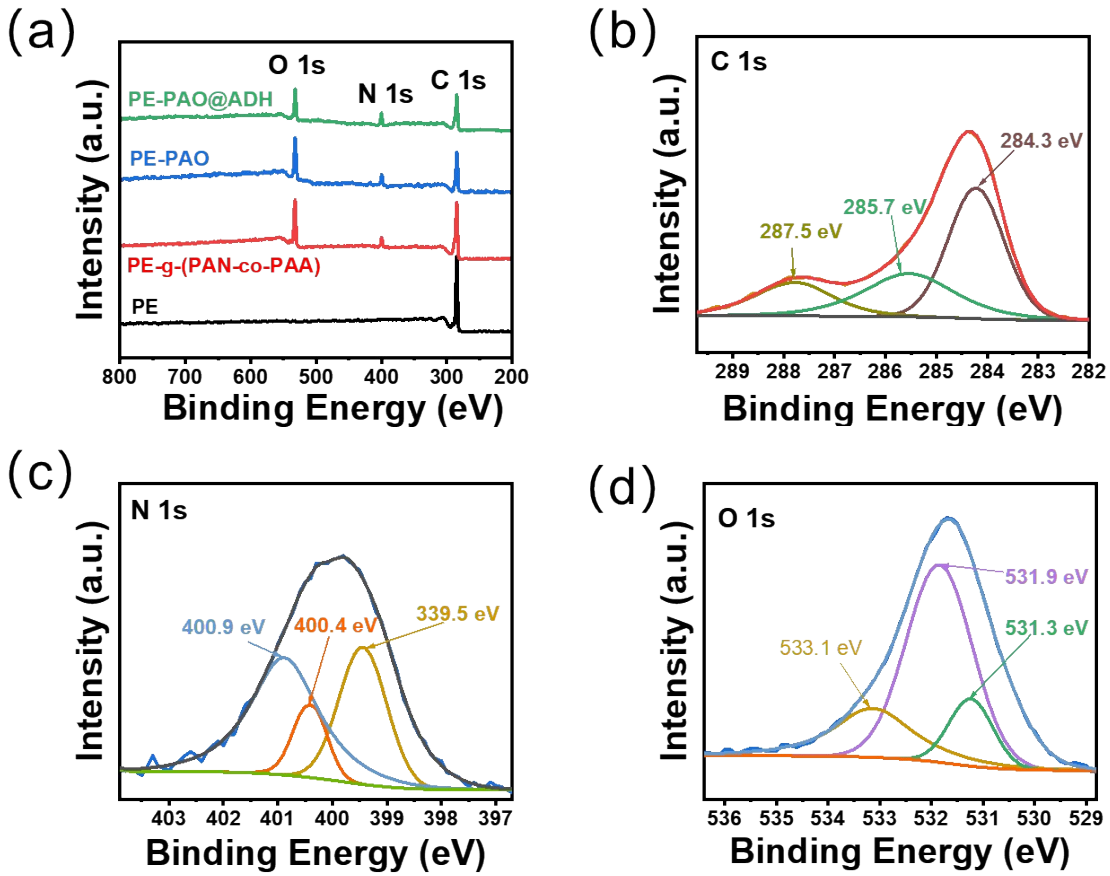

Fig. S5. (a) Survey of the XPS spectra. High-resolution XPS analysis of (b) carbon, (c) nitrogen, and (d) oxygen of PE-PAO@ADH membranes.

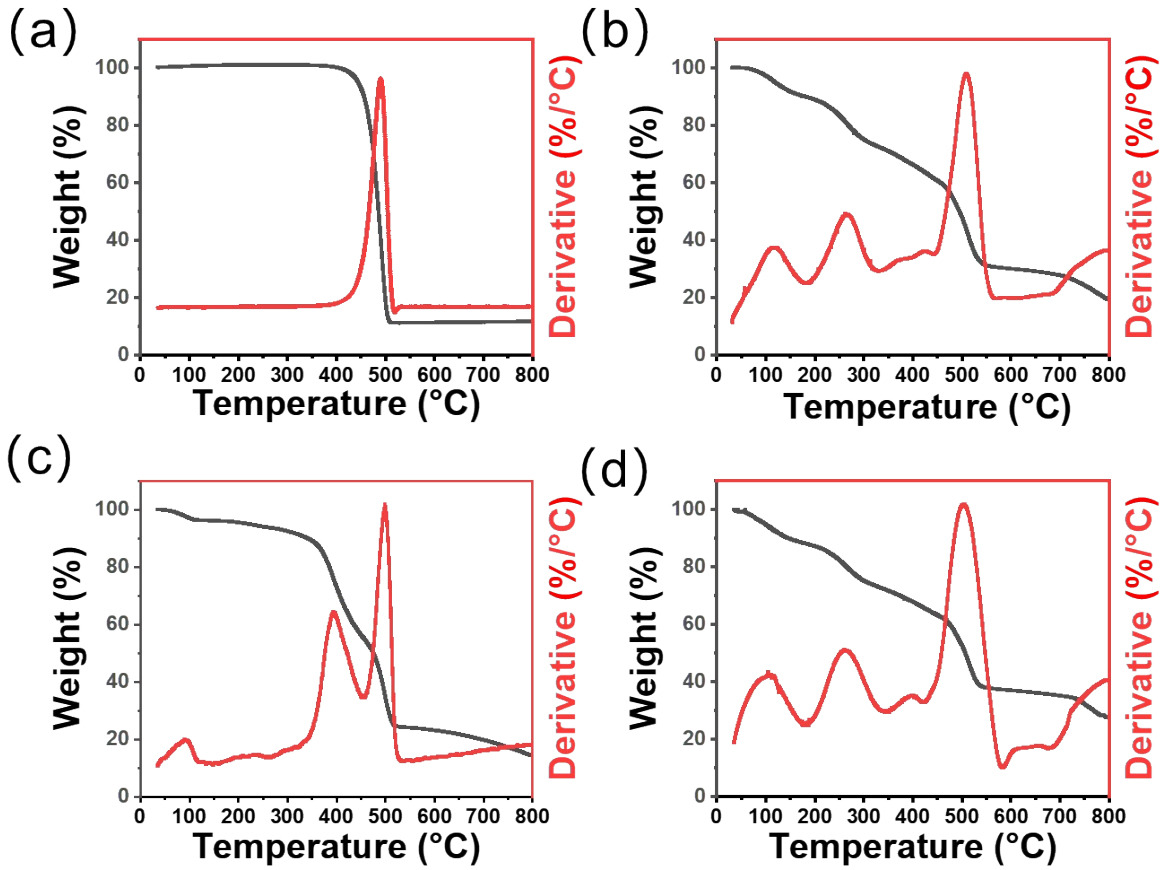

170

171 Fig. S6. TGA and DTG curves of (a) PE, (b) PE-*g*-(PAN-*co*-PAA), (c) PE-PAO, and (d) PE-

172 PAO@ADH membranes in N_2 atmosphere.

173

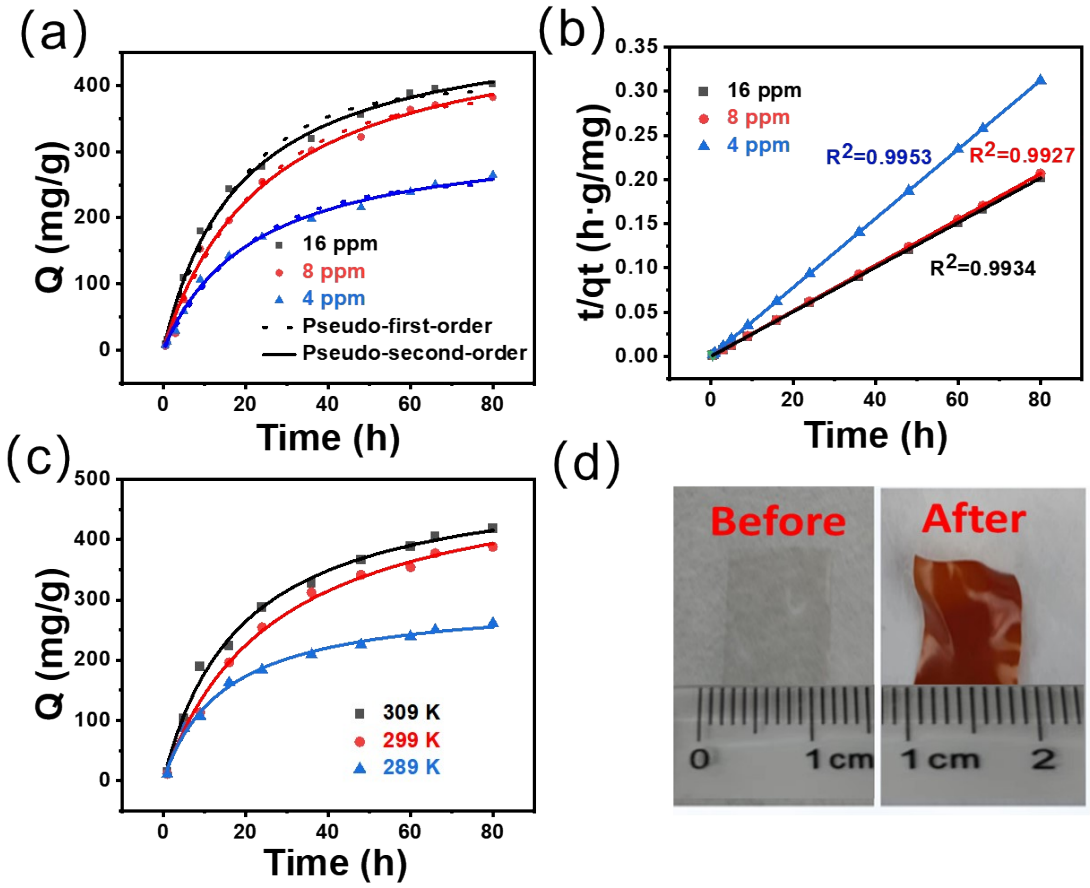

174

175 Fig. S7. Evaluation of uranium adsorption capacity of PE-PAO (a) Kinetic data, and (b)
176 pseudo-second-order models for uranium adsorption by the PE-PAO membrane at different
177 uranium concentrations (4 ppm, 8 ppm and 16 ppm). (c) Uranium adsorption by the PE-PAO
178 membrane at different temperature (289 K, 299 K and 309 K). (d) The PE-PAO membrane
179 before and after adsorption in uranium solution; significant color changes are observed owing
180 to the adsorption of uranium.

181

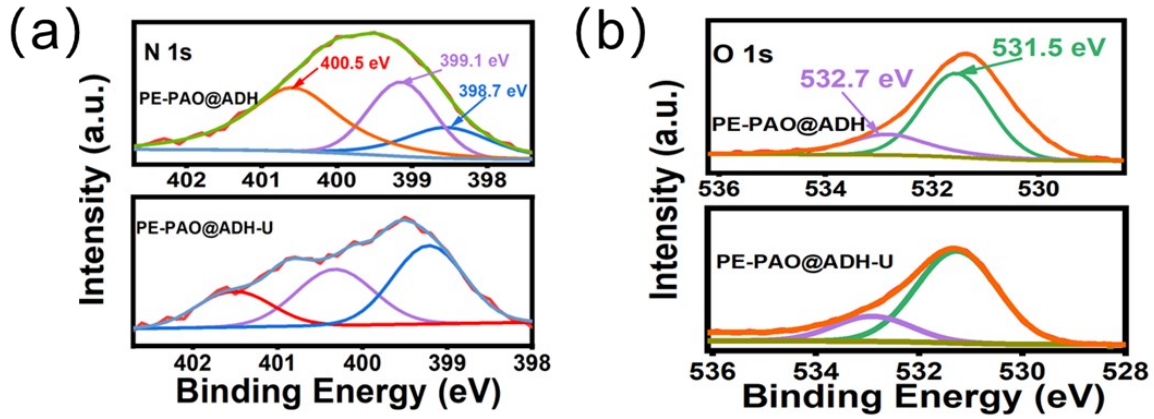

Fig. S8. Adsorption mechanism of PE-PAO and PE-PAO@ADH. (a) N 1s and (b) O 1s XPS spectra of the PE-PAO@ADH before and after adsorption.

3. Supplementary Tables

Table S1. Ion concentration in simulated seawater.

Element	U	V	Fe	Co	Ni	Cu	Zn	Pb	Mg	Ca
Simulated Seawater Conc. in system (ppb)	330	152	141	5.3	101	65	408	34.6	1.2*105	0.6*105

195

196

197 Table S2. The uranium adsorption kinetic fitting parameters of PE-PAO membrane.

Concentration	Pseudo-second-order model			Pseudo-first-order model		
	R^2	q_e (mg-U/g-ads)	K_2 ($g \cdot mg^{-1} \cdot h^{-1}$)	R^2	q_e (mg-U/g-ads)	K_2 ($g \cdot mg^{-1} \cdot h^{-1}$)
4 ppm	0.995	329.3	0.00011	0.989	256.1	0.04795
8 ppm	0.993	508.9	0.00008	0.992	386.8	0.04421
16 ppm	0.993	499.3	0.00014	0.990	396.4	0.05521

198

199 Table S3. Comparison of adsorption capacities in natural seawater among adsorbent materials.

200

Adsorbents	Adsorption from natural seawater		Ref.
	mg-U/g-ads	time(d)	
This work	6.76	30	/
JAEA PE-g-PAO fabric	2.5	56	[20]
PE-g-poly (AO-co-IA)	4.2	56	[46]
PE-g-poly (AO-co-PA)	3.2	56	[47]
PE-g-poly (AO-co-AA)	3.4	77	[48]
PE-g-poly (AO-co-VSA)	3.4	77	[25]
PE-g-poly (AO-co-MA)	3.1	77	[25]
CID NFs	4.8	30	[49]
PAO-BSPE	5.6	33	[8]
AO-OpNpNc	6.3	42	[36]

PIDO nanofiber	8.7	56	[50]

201